



A 900-year New England temperature reconstruction from *in situ* seasonally produced branched glycerol dialkyl glycerol tetraethers (brGDGTs)

Daniel R. Miller^{1,2}, M. Helen Habicht², Benjamin A. Keisling², Isla S. Castañeda², Raymond S. Bradley^{1,2}

5 ¹Northeast Climate Science Center, University of Massachusetts Amherst, Amherst, MA 01003, United States

²Climate System Research Center, Department of Geosciences, University of Massachusetts Amherst, Amherst, MA 01003, United States

Correspondence to: Daniel R. Miller (dmiller@geo.umass.edu)

10

Abstract. Paleotemperature reconstructions are essential for distinguishing anthropogenic climate change from natural variability. An emerging method in paleoclimatology is the use of branched glycerol dialkyl glycerol tetraethers (brGDGTs) in lacustrine sediments to reconstruct temperature but their application is hindered by a limited understanding of their sources, seasonal production, and transport. We report seasonally resolved measurements of brGDGT production within the water column, in catchment soils and in a sediment sequence from a small, deep inland lake in Maine, USA. BrGDGT distributions in the water column are distinct from catchment soils but similar to the distributions in lake sediments, suggesting that (1) brGDGTs are produced within the lake and (2) this *in situ* production dominates the downcore sedimentary signal. Seasonally, depth-resolved measurements indicate that the dominant production of brGDGTs occurs in late fall/early spring and at intermediate depths (18-30 meters) in the water column. We apply these observations to help interpret a 900-year-long brGDGT-based temperature reconstruction and find that it shows similar trends to a pollen record from the same site and to regional and global syntheses of terrestrial temperatures over the last millennium. However, the record also shows higher-frequency variability than has previously been captured by such an archive in the Northeastern United States, potentially attributed to the North Atlantic Oscillation and volcanic/solar activity. This is the first brGDGT- based multi-centennial paleoreconstruction from this region and contributes to our understanding of the production and fate of brGDGTs in lacustrine systems.

15

20

25

1 Introduction

Climate change is one of the most complex and challenging issues facing the world today. The impacts of anthropogenic climate change will likely be exacerbated in heavily populated regions, such as the Northeastern United States (NE US) (Fig. 1), which is comprised of communities that have been historically susceptible to climate change (Horton et al., 2014). Here, over the past 120 years, average temperatures have increased by ~1°C, precipitation has increased by 10%, and sea levels have also risen by ~40 cm (Kunkel, 2013; NOAA, 2014). While historical records document the temperature increase of the past

30



century, they are not long enough to capture the underlying variability of the pre-anthropogenic period. Therefore, high-resolution paleotemperature records, such as those developed from lacustrine sedimentary sequences, are needed to investigate how current climate change compares to long-term natural variability. A regional synthesis of NE US late Holocene climate variability by Marlon et al. (2017) reviews previous temperature reconstructions from terrestrial sediment records using methods such as pollen (Gajewski, 1987; Webb et al., 2003; Oswald et al., 2007), testate amoeba (Clifford and Booth 2013), and leaf wax hydrogen isotopic ratios (Huang et al., 2004, Shuman et al., 2006; Gao et al., 2017). However, these climate proxies may also reflect changes in parameters other than temperature (i.e., precipitation trends, humidity, evapotranspiration, and vegetation changes) (Gajewski 1988; Hou et al., 2008; Marlon et al., 2017). Therefore, additional quantitative paleotemperature records are needed to accurately assess the history of temperature variations in this region (Marlon et al. 2017).

Branched glycerol dialkyl glycerol tetraethers (brGDGTs), found globally in lakes, soils, rivers, and peats, provide an independent terrestrial paleothermometer well-suited to this task (e.g. Weijers et al. 2007; Peterse et al. 2012; De Jonge et al. 2013). BrGDGTs are comprised of two ether-linked dialkyl chains containing zero to two methyl branches (prefixes I, II, and III) and zero to two cyclopentane moieties (suffixes a, b, and c). Although the source organisms are unknown, the compounds are thought to be bacterial membrane lipids (e.g., Sinninghe Damsté et al., 2011). Noting a strong correlation between mean annual air temperature (MAAT) and the distribution of brGDGTs in global soils, Weijers et al. (2007) proposed that sedimentary brGDGTs could be used as a proxy for past soil temperature, which in many cases is similar to mean annual air temperature. This motivated the development and later refinement of two indices, based on the degree of methylation and cyclization of brGDGTs (MBT and CBT), which are used to reconstruct past climate (e.g. Weijers et al., 2007, Peterse et al., 2012, De Jonge et al., 2013).

Initially, brGDGTs were presumed to be exclusively produced in soils, and subsequently washed into lakes or marine environments via erosion by rivers and streams (Hopmans et al., 2004). Further research has indicated these compounds are also produced *in situ* in lakes and rivers (e.g. Bechtel et al., 2010; Buckles et al., 2014; De Jonge et al., 2015; Loomis et al., 2012; Schoon et al., 2013; Tierney et al., 2010; Tierney and Russell, 2009; Zell et al., 2013; Zhu et al., 2011). Although some studies suggest that distinct brGDGTs are produced within the water column of lakes (Weber et al., 2015; Colcord et al., 2015) and show that their production is seasonally biased (Loomis et al., 2014), relatively limited work has been done to understand their in-situ production and its consequences for the sedimentary brGDGT record (Zhang et al., 2016). Knowledge of brGDGT production and seasonality is important for appropriately calibrating and understanding downcore records, yet to date little to no studies have combined modern observations of brGDGT distributions in the environment with a paleoclimate reconstruction for a temperate lake system.

Here we examine brGDGT abundances and distributions in catchment soil samples and at varying depths in the water column throughout the year at an inland lake in Maine, NE US (Fig. 1). We collected samples from 2014–2015 to assess the seasonality and location of brGDGT production in and around Basin Pond, ME. We then applied our observations to the



interpretation of a 900 year- long relative temperature record, providing the first decadal-resolved brGDGT-derived lacustrine paleoclimate reconstruction for this region.

2 Site information, field sampling, and laboratory methods

2.1 Study Site

- 5 Basin Pond, located in Fayette, ME (44° 28' N, 70° 03' W, elevation 124 m above sea level), is a small, deep lake with an area of 0.14 km² and a maximum depth of 32.6 m (Fig. 1). Basin Pond is fed from groundwater and precipitation, with one small, dammed, outlet stream running westward into the adjacent David Pond (Frost, 2005). Most of the 0.53 km² catchment area is dominated by a well-developed deciduous hardwood and evergreen forest, with only one residential building. Mean annual air temperature at Basin Pond is ~5.9°C and average annual precipitation is ~1150 mm (NOAA, 2014).
- 10 Basin Pond contains a unique sedimentary sequence comprised of annual laminations (varves) due to permanent water column stratification (Wetzel, 1983; Frost, 2005) resulting from a persistent thermocline. This stratification causes permanent bottom water anoxia, which enhances the preservation of annual laminations throughout the record (O'Sullivan, 1983). The Basin Pond varves are biogenic, with couplets comprised of a lighter, diatom-rich summer layer and a darker, humic winter layer (Frost, 2005).

15 2.2 Sediment Coring

- Sediment coring was performed from ice (in March 2014) in the deepest part of the lake at 32 m (44° 27' 27" N, 70° 03' 09" W) using a UWITEC gravity coring system. Core BP2014-3D (52 cm) captured an undisturbed sediment-water interface and was subsampled in the field at 0.5 cm resolution for radioisotopic dating. Core BP2014-5D (174 cm) was immediately capped upon retrieval. Cores were split, photographed, and non-destructive down-core logging was performed using an Itrax XRF
- 20 core scanner with a Molybdenum tube at 100 µm resolution in the Department of Geosciences at University of Massachusetts Amherst. Cores were kept refrigerated until analysis.

2.3 Sediment trap construction, deployment and retrieval

- Sediment traps were designed and constructed at University of Massachusetts Amherst. Sediment trap collection cones were made of high density polyethylene (HDPE), with a diameter of ~1 m (Fig. 1), and attached to 4L bottles for the settling
- 25 particulate matter (SPM) collection (Fig. 1). Note that our definition of SPM includes both material suspended in the water column and settling into the traps. Five sediment traps were deployed on May 27, 2014 at 6, 12, 18, 24, and 30 m depths in the deepest part of the lake (Fig 2). SPM was collected from all traps on 7/2/14, 8/16/14, 9/14/14 and 6/5/15. Each trap continuously accumulated SPM from deployment until collection and therefore each sample represents material collected over 36, 40, 28, and 264 days, respectively. Thus, samples collected on a given date represent the previous month (or longer) of



sedimentation. Catchment soil samples were also taken around the perimeter of the lake at the time of initial trap deployment. All soil and water SPM samples were kept frozen until analysis.

3 Methods

3.1 Sedimentary Age Model

- 5 Subsamples for downcore climate reconstruction were taken every 0.5 cm from the uppermost 68 cm of BP2014-5D. The age model for this core is based on ^{210}Pb , varve counts, and five ^{14}C dates and was previously published by Miller et al., (2017). The sediment examined here ranges in age from modern to ~1100 BP (Miller et al., 2017).

3.2 Laboratory Methods

Overall, 5 catchment soil, 19 SPM sediment trap samples, and 136 sediment core samples were analyzed. Soil and lake
10 sediment samples were freeze-dried and homogenized prior to extraction. For SPM samples, water from each collection bottle was filtered through a 47mm, 0.3- μm combusted Sterlitech glass fiber membrane filter, and dried prior to extraction. For most samples, a total lipid extract (TLE) was obtained using a Dionex Accelerated Solvent Extractor (ASE 200) with a mixture of dichloromethane (DCM)/ methanol (MeOH) (9:1, v/v). For four SPM samples, plastic filters were washed and sonicated with HPLC-grade water, which was subsequently extracted with DCM three times to avoid contamination. The TLE from SPM and
15 catchment soil samples was separated into apolar (9:1 DCM/hexane v/v) and polar (1:1 DCM/MeOH v/v) fractions, while the lake sediment samples were separated into apolar, ketone (1:1 hexane/DCM) and polar fractions using alumina oxide column chromatography. For all samples, one half of each polar fraction was filtered through 0.45 μm PTFE syringe filters using 99:1 hexane/isopropanol (v/v). 0.1 μg of C_{46} GDGT internal standard was added to each polar fraction prior to analysis. The other half of each polar fraction was derivatized using bistrimethylsilyltrifluoroacetamide (BSTFA), and algal biomarkers were
20 identified with a Hewlett-Packard 6890 Series gas chromatograph coupled to an Agilent 5973 mass spectrometer (GC-MS) using a Restek Rtx-5ms (60m x 250 μm x 0.25 μm) column. Algal biomarkers were quantified with an Agilent 7890A dual gas chromatograph-flame ionization detector (GC-FID) equipped with two Agilent 7693 autosamplers and two identical columns (Agilent 19091J-416: 325 $^{\circ}\text{C}$: 60m x 320 μm x 0.25 μm , HP-5 5% Phenyl Methyl Siloxan). For both the GC-MS and GC-FID, Helium was used as the carrier gas. The ovens began at a temperature of 70 $^{\circ}\text{C}$, increased at 10 $^{\circ}\text{C min}^{-1}$ to 130 $^{\circ}\text{C}$, increased
25 again at 4 $^{\circ}\text{C min}^{-1}$ to 320 $^{\circ}\text{C}$, and then held for 10 minutes. Compounds were quantified using an external calibration curve where squalane was injected at multiple concentrations ranging from 2 to 100 ng/ μl , r^2 values for linearity tests were >0.99.

3.3 brGDGT analysis

Polar fractions were analyzed on an Agilent 1260 high performance liquid chromatograph (HPLC) coupled to an Agilent 6120
30 Quadrupole mass selective detector (MSD). Separation of compounds was achieved using the UHPLC method of Hopmans et al. (2016). The technique uses two Waters UHPLC columns in series (150 mm x 2.1 mm x 1.7 μm) and isocratically elutes



brGDGTs using a mixture of hexane (solvent A) and hexane: isopropanol (9:1, v:v, solvent B) in the following sequence: 18% B (25 minutes), linear ramp to 35% B (25 minutes), linear ramp to 100% B (30 minutes). Mass scanning was performed in selected ion monitoring (SIM) mode. brGDGTs were quantified with respect to the C₄₆ standard, assuming equal ionization efficiency for all compounds. For calculation of MBT_{5ME}, CBT_{5ME}, and the Isomer Ratio (IR), the following equations were

5 used:

$$\text{MBT}'_{5Me} = \frac{\text{Ia} + \text{Ib} + \text{Ic}}{\text{IIa} + \text{IIb} + \text{IIc} + \text{IIa}' + \text{IIb}' + \text{IIc}' + \text{Ia} + \text{Ib} + \text{Ic}} \quad (1)$$

$$\text{CBT}'_{5Me} = -\log \left(\frac{\text{Ib} + \text{IIb}}{\text{Ia} + \text{IIa}} \right) \quad (2)$$

$$10 \text{ IR} = \frac{\text{IIa}' + \text{IIb}' + \text{IIc}' + \text{IIIa}' + \text{IIIb}' + \text{IIIc}'}{\text{IIa} + \text{IIa}' + \text{IIb} + \text{IIb}' + \text{IIc} + \text{IIc}' + \text{IIIa} + \text{IIIa}' + \text{IIIb} + \text{IIIb}' + \text{IIIc} + \text{IIIc}'} \quad (3)$$

3.4 Time Series Analysis

To analyze the variance in the data presented here, we used the *Astrochron* R package (Meyers, 2012). Pre-processing of the data was kept to a minimum to avoid introducing spurious signals. The downcore brGDGT reconstruction was re-interpolated to 7-yr resolution (equivalent to median resolution of the raw data, see results) prior to spectral analysis. The published
 15 PAGES2k datasets were analyzed with their published chronologies, which is 1 year resolution for most regions and 10 years for the North American tree-ring based reconstruction (PAGES2k, 2013). Each of these reconstructions were smoothed to 7 year averages for easier comparison to our record.

4 Results

4.1 Catchment Soils

20 BrGDGTs Ia and IIa dominated distributions in the catchment soil samples, with relative abundances of 65% ±13% and 28% ±7%, respectively (Fig. 2). The next largest relative abundances were IIIa and Ib, comprising 3% ±6% and 3% ±1%, respectively (Fig. 2).

4.2 SPM

25 BrGDGTs Ia, IIa and IIIa dominated distributions in the SPM samples, with relative abundances of 28% ±8%, 37% ±7%, and 30% ±8%, respectively (Fig. 2). The next largest relative abundances were Ib and IIb, each comprising 2% ±<1%. Through the four collection periods, the distributions are relatively consistent. However, in July and August 2014, group I brGDGTs were the most abundant, whereas in September 2014 and June 2015 reductions in group I brGDGTs were accompanied by increases in group 3 brGDGTs (Fig. 2). Overall, fluxes of brGDGTs were highest in September 2014 (0.36 to 15.2 ng m⁻² day⁻¹).



¹⁾ (Fig. 3). In July and August 2014, brGDGT fluxes ranged from 0.009 to 0.04 ng m² day⁻¹ and 0.04 to 0.14 ng m² day⁻¹, respectively (Fig. 3). In general, summed brGDGT fluxes increase with depth, with up to an order of magnitude higher fluxes at 30 m compared to 6 m (Fig. 3).

BrGDGT fluxes and distributions also varied as a function of depth (Fig. 4,5). BrGDGT fluxes in the upper and lower water column peaked in September with fluxes of 0.4 to 0.6 ng m² day⁻¹ and 7 to 16 ng m² day⁻¹, respectively. The average distributions also changed as a function of depth. Group I brGDGTs comprised 30% of the distributions at all depths. Group II brGDGTs had the greatest abundance at 12 and 18 m water depth (Fig. 5), comprising up to 50% of the distribution. Group III brGDGTs peaked at 30 m, comprising 35% of the distribution, and showed a minimum at 18 m of <20%. These distributions lead to variations in MBT[']_{SME} and CBT[']_{SME} indices as a function of depth (Fig. 5). MBT[']_{SME} varied from 0.34 to 0.46, and peaked at 24 m water depth (Fig. 4). CBT[']_{SME} varied from 1.1 to 1.6, peaked at 12 m and then decreased with depth (Fig. 4).

4.3 Sediment samples

To represent surface sediments, we averaged the measurements from the uppermost 5 cm of Core BP2014-5D, corresponding to approximately 35 years (Miller et al., 2017). BrGDGTs Ia, IIa, and IIIa dominate the distribution, with relative abundances of 27%, 32%, and 33%, respectively (Fig. 3). The next largest relative abundances were IIb, Ib, and IIIb (3%, 2%, and 1%, respectively). Reconstructed MBT[']_{SME} values in surface sediments ranged from 0.35 to 0.45 (Fig. 6).

4.4 BrGDGT isomer ratios

The chromatographic separation of brGDGTs allows for the separation of penta- and hexa-methylated brGDGT isomers, and improves the error associated with temperature reconstruction (DeJonge et al., 2013; DeJonge et al., 2014). Analysis of the relative abundances of these isomers has also been used to identify different production sources of brGDGTs (DeJonge et al., 2014; Weber et al., 2015). The summed IR for soils, lake water and sediments at Basin Pond were significantly different. The IR value for soils averaged 0.03, while the water samples and sediments averaged 0.26 and 0.30, respectively (Fig. 6).

4.5 Downcore reconstruction

Sampling every 0.5 cm in Core BP2014-5D yielded a record of brGDGT distributions with a resolution of 4 to 13 years (median: 7). brGDGT concentrations in these samples ranged from 1.16 to 21.07 (median: 8.09) μg g^{sed}⁻¹. MBT[']_{SME} ranged from 0.34 to 0.50 (median: 0.39). MBT[']_{SME} values fluctuate around a stable mean from 1100-1400 AD, then broadly decrease from ~1400 AD until the present day (Fig. 7). Decadal variability is superimposed on the long-term decreasing trend (Fig. 7). Prominent, multi-decadal low-MBT[']_{SME} events are apparent from 1420–1444, 1500–1520, 1593–1627, 1762–1829, and 1908–1950 (Fig. 7). Multidecadal high-MBT[']_{SME} events are observed from 1261–1283, 1317–1351, 1556–1583, 1632–1657, 1829–1846 and 1958–1987 (Fig. 7).



5. Discussion

5.1 Calibration of the brGDGT paleothermometer

Several lacustrine brGDGT calibrations have been developed (Tierney et al., 2010; Pearson et al., 2011; Sun et al., 2011; Loomis et al., 2012) following strong evidence for *in situ* brGDGT production (e.g. (Tierney and Russell, 2009; Buckles et al., 2014; Loomis et al., 2014). Unfortunately, these are generally either based on relatively few samples (e.g. Zink et al., 2010; Loomis et al., 2012) or are geographically restricted (e.g. Tierney et al., 2010; Foster et al., 2016). Furthermore, under new chromatographic separation schemes (Hopmans et al., 2016), pH no longer affects MBT values (De Jonge et al., 2014) and few lacustrine calibrations have been developed using this new method. Recently, a calibration was developed for African lakes using only the 5 methyl brGDGTs. However, we do not believe it is appropriate to apply an African calibration to lakes in the NE US, as these two regions are climatically different and their lakes differ in terms of stratification/mixing. We thus present our results simply in terms of the MBT'_{SME} index, which we note shows a strong positive correlation with temperature in all previously published global calibrations (i.e. Weijers et al., 2007; Peterse et al., 2012; De Jonge et al., 2013) and the new African lakes calibration (Russell et al., 2018) as well as in the data we present here (see Supplementary Materials).

5.2 In situ and seasonal production of brGDGTs in Basin Pond

Multiple lines of evidence suggest that brGDGTs deposited in Basin Pond sediments are predominantly produced within the water column. First, we observe significant differences in the fractional abundances of brGDGTs between soil, SPM and lake sediments (Figs. 2, 5), suggesting *in situ* production occurs in both soil and lacustrine environments. Average distributions of brGDGTs reveal that lake sediments and SPM are similar in Ia and IIIa content, while the soils differ substantially (Figs 2, 5). The relative amounts of 5- and 6-methyl brGDGTs also differs between soils and lake water and sediment (Figs 2, 5), and as seen in the average IR values (Fig. 6). MBT'_{SME} and CBT values for lake sediment and soils are different, while SPM samples lie between the respective end members, consistent with *in situ* production within Basin Pond and mixing with soil brGDGTs (Fig. 6). The degree of cyclization (mean CBT = 1.2) is significantly higher in lake sediments than in soil samples (mean CBT = 1.5) (p value = 0.021 from two-tailed t-test), and brGDGTs are more methylated (p value = 0.003) in lake sediments (mean MBT'_{SME} = 0.38) than in soils (mean MBT'_{SME} = 0.7) (Fig. 6). This agrees with differences in brGDGT distributions recorded in other temperate (Tierney et al., 2012; Wang et al., 2012; Loomis et al., 2014) and tropical (Tierney and Russell, 2009; Loomis et al., 2011; Buckles et al., 2014) lakes and catchment area soils, and suggests *in situ* production of relatively more cyclized and methylated brGDGTs within lakes.

Monthly variations in fluxes and distributions of brGDGTs also suggest lacustrine brGDGTs have an *in situ* source. Fractional abundances of brGDGTs vary as a function of depth suggesting brGDGTs in SPM may respond to (and record) temperatures at different depths. Although seasonal precipitation events leading to soil erosion have previously been invoked to explain increased seasonal brGDGT fluxes (Sinninghe Damsté et al., 2009; Vershuren et al. 2000), fluxes of brGDGTs are not higher during summer months, when strong precipitation events generally occur at Basin Pond (NOAA, 2014). Furthermore, SPM



samples maintain the distinct lacustrine fractional abundance distribution, suggesting they are not significantly influenced by a flux of terrestrially derived brGDGTs from runoff (Fig. 2). Instead, brGDGT fluxes are orders of magnitude higher in September (Fig. 3). BrGDGT fluxes at all depths are generally low throughout the summer months (June–August). A large flux increase at depth (18–30 m) occurs during September. BrGDGT distributions in SPM generally do not reflect that of the surrounding soils, suggesting that there is no significant flux of brGDGTs into the lake from either summer storm erosion or spring freshet runoff. Permanent lake stratification likely prevents resuspension, thus limiting any transfer of brGDGTs from greater depths to the upper water column. Overall, this suggests an annual seasonal production of brGDGTs in Basin Pond, with a fall bloom occurring at intermediate (18–30 m) depths. Therefore, brGDGT temperatures recorded in the lake sediments likely reflect a seasonally biased (fall), rather than mean annual, temperature. We observe the following: (1) peak brGDGT flux is observed at 18–24 m water depth, suggesting that the organisms producing the most brGDGTs thrive in the mid to upper water column (Fig 3); (2) peak brGDGT production occurs in September, suggesting that the sedimentary record will be biased toward brGDGTs produced during this period (Fig 3); And (3) for the four time-periods sampled, brGDGT distributions (as described by MBT'_{SME}) correlate with temperature (Fig S1). Interestingly, at 18–24 m depth the water temperature shows little to no seasonal cycle, remaining at approximately 4 °C for the entire year. Therefore, if maximum brGDGT production is indeed occurring here, it is possible that another parameter, which covaries with temperature on a seasonal scale (i.e. light duration, water chemistry, nutrient availability), may drive, or contribute to, the distribution of brGDGTs produced at depth at Basin Pond.

Although few studies are available for comparison, Loomis et al. (2014) studied brGDGT in another temperate lake in the NE US (Lower King Pond, Vermont). Whereas brGDGT production in Lower King Pond peaked during fall and spring, it was linked to seasonal mixing events, which do not occur at Basin Pond. Moreover, Basin Pond is ten times bigger by area and four times deeper than Lower King Pond. Similar to Lower King Pond, brGDGT production at Basin Pond seems to be seasonal, and calibration of brGDGTs against seasonal (in this case, fall) temperatures is necessary to accurately reconstruct past temperature change for this location. If the behavior of brGDGTs in Lower King Pond and Basin Pond is representative of all temperate lakes, then calibration to fall or spring temperature may be the most appropriate choice for these settings. While we believe that the MBT'_{SME} trends in our brGDGT-based reconstructions reflect temperature change, future work is necessary to generate properly calibrated (and accurate) paleotemperature records.

5.3 Downcore brGDGT Reconstructions

Based on the contents of the sediment traps, we argue that the downcore brGDGT reconstruction is likely weighted toward September temperature change in the NE US over the last ~900 years. We note that brGDGTs are present at all depths measured but peak at 24–30 m depth, indicating that the compounds reaching the sediment represent an integrated signal from the entire water column. Although brGDGT concentrations vary down core, they are not correlated with reconstructed MBT'_{SME} values ($p=0.25$), indicating that brGDGT production and MBT'_{SME} variability are largely decoupled. The average reconstructed MBT'_{SME} value over the last 100 years is 0.37. At the beginning of the record (AD 1100), MBT'_{SME} values are ~0.4 (Fig. 7).



Values increase until AD 1340, reaching a maximum of 0.5 (Fig. 7). Multi-taper method spectral analysis reveals significant power at periodicities of 80, 63, and 47 years (Meyers, 2012). MBT'_{5ME} values decrease from AD 1340 to AD 1900 with variability of ± 0.05 superimposed on this trend.

5.4 Comparison to Regional Hydroclimate Records in the NE US

- 5 Regional hydroclimate has been reconstructed at several sites on similar timescales as the Basin Pond record. We find that while similarities exist between our record and these hydroclimate records, the Basin Pond MBT'_{5ME} record shows long-term changes that are not observed in other regional reconstructions. The MBT'_{5ME} record infers an overall cooling from ~ 1300 AD to ~ 1900 AD (Fig. 7), which is observed in pollen-derived temperature reconstructions from Basin Pond (Gajewski 1988), although we note that there may be a difference in seasonality between pollen reconstructions and MBT'_{5ME} from Basin Pond.
- 10 The greatest flux of brGDGTs occurs during September, whereas the published pollen data record reflects summer (JJA) temperature. Despite these differences in seasonality, the two records broadly agree. The long-term cooling trend is also observed in a hydrogen isotope-based temperature reconstruction from Little Pond, Massachusetts (Gao et al., 2017). Although the timing of maximum temperatures at that site occurs later than at Basin Pond, both records show the coolest part of the last 900 years occurring at ~ 1850 AD (Fig. 7).
- 15 A potential cause for the discrepancy between the Basin and Little Pond records is that the latter is based on hydrogen isotopes from leaf waxes, which represent an integrated signal of temperature and hydrological change. Bog records provide additional, high-resolution reconstructions of hydrological conditions in the NE US over this time period via analysis of testate amoeba (a proxy for water table depth) and the *Sphagnum*/Vascular Ratio (SVR) (Clifford and Booth, 2013; Nichols and Huang, 2012). The testate amoeba records show that the last 400 years (i.e., 1600–2000 AD) have been generally wetter than the preceding
- 20 400 years (1200–1600 AD). However, unlike the temperature reconstructions, these records do not show a long-term linear trend (Fig. 7).
- These observations are surprising given the record of fire history at Basin Pond (Miller et al., 2017), which shows five periods of increased charcoal deposition since 1100 AD (Fig. 7). It is important to note that wildfire activity is a complex phenomena, with multiple factors affecting fire occurrence apart from climate variability in the NE US (Marlon et al. 2017). However, our
- 25 data suggest that fire activity in the NE US may be influenced more by shorter-term (multi-decadal) variations in climate, particularly seasonal cooling superimposed on dry conditions, as opposed to longer-term, multi-centennial climate trends. Surprisingly, the first 200 years of the record (1100–1300 AD) are dominated by warm and dry conditions, but no fire events were recognized during this period. Three events, between ~ 1300 and ~ 1700 , are associated with regionally dry conditions. Although average Basin Pond MBT'_{5ME} values are higher on a multi-centennial time-scale during this time period, the fire
- 30 events themselves occur synchronously with multi-decadal cold intervals. Two recent fire events occurred during the historical period which is reconstructed as relatively cool and wet. We suggest these fires to be less climatically driven and are perhaps more strongly associated with human disturbance.



5.6 Comparison with Northern Hemisphere Records

A compilation of Northern Hemisphere temperature records for the last 2000 years reveals sustained warmth from AD 830–1100, just prior to the beginning of our reconstructions (PAGES2k, 2013) (Fig. 8). Northern Hemisphere climate then entered a cooler phase, though the timing of this transition varied regionally between AD 1200 and 1500 (PAGES2k, 2013). North American pollen data, as well as pollen data from Basin Pond, show elevated, though decreasing, temperatures through AD 1500 (Gajewski, 1988; PAGES2k, 2013) (Fig. 8). Surprisingly, the brGDGT MBT_{SME} values are better correlated with regional tree-ring records and compilations of European and Arctic temperatures, which all show warm anomalies, followed by cooling, earlier this century. Thus, the multi-centennial structure of the brGDGT record from Basin Pond is supported by other local, regional, and global records (PAGES2k, 2013). On a multi-decadal scale, there is variability potentially associated with volcanic events recognized as having a global impact. Five intervals during the last millennium were defined as ‘volcanic-solar downturns’: AD 1251–1310, 1431–1520, 1581–1610, 1641–1700, and 1791–1820 (PAGES2k, 2013). All but the most recent (1908–1950) of the cool events are present in the Basin Pond MBT_{SME} record (Fig. 8).

There is some similarity between the Basin Pond reconstruction and other northern hemisphere reconstructions (PAGES2k, 2013) in that we note cooling (low MBT_{SME} value) events during (or within age model uncertainty of) five prominent volcanic downturns that occurred during the last millennium (PAGES2k, 2013) (Fig. 8). The brGDGT record is also peppered with warm (high MBT_{SME}) anomalies; many of these seem to be coherent with tree-ring based reconstructions of North American climate (i.e. AD 1300, 1550, 1830) and are sometimes associated with negative phases of the NAO (Fig. 8). The sensitivity of the Basin Pond sediment record to regional scale climatic variations is highlighted by time series analysis. Multispectral taper method analysis reveals a persistent cycle in the brGDGT-based temperature reconstruction with a period of 57–63 years (Fig. 8). The Northern Hemisphere tree-ring compilation also shows a cyclicity with a period of 60 years (Fig. 8). However, the fact that the two datasets are not significantly correlated indicates the variability at 60-year periods is not exactly in-phase over the 900 year period covered by the two records. Cross-correlation analysis indicates that the correlation between the two datasets is strongest when the tree-ring reconstruction is lagged by 42 years relative to the Basin Pond temperature record ($r=0.33$, $p=0.04$). Significant spectral peaks with a similar period exist in the annually-resolved records from Europe (period = 65 yr), Asia (period = 58 yr) and the Arctic (period = 58 yr) (PAGES2k, 2013). However, the same analyses applied to South American, Australasian, and Antarctic reconstructions do not show spectral peaks at this period (PAGES2k, 2013). Thus, it appears that the Basin Pond brGDGT record captures variability that is representative of, but not necessarily in-phase with, the Northern Hemisphere at large. One possible mechanism to explain this is the North Atlantic Oscillation (NAO), which exhibits a quasi-periodic oscillation of ~60 yr (Sun et al., 2015). While the NAO has some regionally coherent climatic effects, the signature of positive and negative NAO modes is spatially heterogeneous and complex; this could explain the phase offset in the ~60 yr band between the Basin Pond record and the other Northern Hemisphere reconstructions.

Another possible driver of the MBT_{SME} changes we see is the Atlantic Multidecadal Oscillation (AMO). The AMO is based sea surface temperature anomalies in the North Atlantic and shows variability in quasi-periodic 60–80 yr cycles (Trenberth et



al. 2017). An AMO reconstruction spanning the last 400 years shows some similarities to the MBT'_{SME} reconstruction from Basin Pond. Although the records do not show a strong cross correlation, they feature apparently synchronous cool and warm periods (i.e. 1550 to 1650 and 1780 to 1830) (Fig. 8). This suggests that climate at Basin Pond is coupled to Atlantic sea surface temperatures on multi-decadal timescales. Thus, the record presented here may prove useful in the future for reconstructing changes in the AMO earlier in the paleorecord.

5.7 20th century Meteorological station and Maine statewide temperature data

Daily temperature measurements from meteorological stations located within 32 kilometers of Basin Pond were accessed through the National Climatic Data Center (NOAA, 2014). To ensure maximum temporal coverage, daily records from two stations (Farmington and Livermore Falls) were compiled, with Farmington covering 1893–2002, and Livermore Falls covering 2002–2014. These data formed a nearly continuous and complete 121 year record of observational data from October of 1893 to December 2014 (NOAA, 2014) (Fig. 9). Furthermore, statewide and regional average temperatures for Maine were obtained from 1895–present day and compared to the local temperature station data (NOAA, 2014) (Fig. 9).

Average temperatures in Maine have warmed by ~1.5°C since 1895 (Fig. 9). Although this trend is apparent in all seasons, it is smallest during the spring. The temperature increase is dominated by changes from 1895-1945 and 1985-present; for the forty intervening years mean temperatures were more stable, with a slight cooling observed during fall (Fig. 9). Interannual variability of +/- 1°C is observed throughout the record, with the most pronounced variability during the winter (NOAA, 2014). Local meteorological observations from Farmington, ME show similar structure to the statewide trends, but differ substantially enough, especially in the last fifty years, that we consider them inaccurate and use the state averages for further comparison.

5.8 20th Century brGDGT Reconstructions

Variations in MBT'_{SME} values for the last 100 years do not agree with instrumental observations. The brGDGT-based reconstruction shows stable values from 1900-1950, followed by an abrupt increase in MBT'_{SME} of 0.1 over two decades (three data points), which decreases again over the subsequent two decades (three data points) (Fig. 9). This produces a prominent spike that is irreconcilable with instrumental records. In fact, instrumental records indicate a slight cooling, or at least a stabilization of warming, starting at the same time when the MBT'_{SME} values begin to increase (Fig. 9). Low MBT'_{SME} values in surface and core top sediments have been noted in other studies as well (Sinnighe Damsté et al., 2012; Tierney et al., 2012), suggesting this trend is reproducible in different regions and environments, and may be driven by mechanisms associated with brGDGT production or preservation.

It is possible that land-use change and other anthropogenic impacts have had an impact on the brGDGT record over the last 100 years. However, known land use change in the Basin Pond catchment is minimal over the past century (Gajewski, 1988). A complicating factor is the addition of the piscicide rotenone to the lake in 1955 to remove fish species in competition with trout (USGS, 1996). While the estimated lifetime of rotenone in the water column is short (days to weeks), it has been shown



to have lasting long-term (years) effects on zooplankton communities and lake productivity (Kiser, 1963; Andersen, 1970; Sanni and Waervagen, 1990).

In lacustrine environments, some classes of lipid biomarkers, specifically sterols and stanols, can give valuable insight into variability of lake productivity of certain types of algae throughout time. Many sterols (and their saturated counterparts, stanols) can be indicative of certain groups of source organisms, in particular, specific phytoplankton groups (Castañeda and Schouten, 2011; Volkman, 2003; Volkman et al., 1998). For example, dinosterol and dinostanol are found in dinoflagellates and are not produced in higher plants, and are therefore used as a biomarker for dinoflagellate species (Volkman et al., 1998). The phytosterol class, including β -sitosterol/stanol and campesterol/stanol, has been linked to terrestrially-derived higher plant sources (Fernholz and MacPhillamy, 1941; Segura et al., 2006; Volkman, 2003, 1986). The compounds isololiolide and loliolide are known to be anoxic degradation products of diatoms, and have been used as a biomarker for diatom species (Klok et al., 1984; Repeta, 1989). Long-chain alkyl diols are produced by eustigmatophyte or yellow-green algae, and can be indicative of this algal class (Volkman et al., 1998). At Basin Pond, several algal community biomarker concentrations, including isololiolide/loliolide, dinosterol/stanol, and C_{30} 1,13 *n*-alkyl diol, decrease following the rotenone treatment in 1955 while B-sitosterol increases (Fig 9) suggesting a shift in the overall algal community structure. Additionally, after 1955 contributions of the different algal biomarkers are remarkably stable in comparison to earlier times (Fig 9). Thus, we believe that while the Basin Pond record may be useful for describing regional climate evolution over the last millennium in the NE US, it may have been compromised over the 20th century by anthropogenic influences, a fate that is not uncommon for lakes in developed regions (Itkonen & Salonen 1994, Köster et al., 2005, Myrbo, 2008).

6 Conclusions

We find evidence for seasonally-biased, *in situ* production of branched glycerol dialkyl glycerol tetraethers (brGDGTs) in a lake in central Maine, NE US. BrGDGTs are mostly produced in September at Basin Pond, and their downward fluxes in the water column peak at 24 m water depth. A downcore brGDGT-based reconstruction reveals both gradual and transient climate changes over the last 900 years and records cooling and warming events correlated with other Northern Hemisphere records and the NAO and AMO indices. This suggests inland Maine climate is sensitive to hemispheric climate forcing as well as changes in regional atmospheric pressure patterns and North Atlantic sea surface temperatures. Along with a pollen record from the same site, our reconstruction reveals a prominent cooling trend from AD 1100–1900 in this area. Comparison with regional hydroclimate records suggests that despite increasingly cool and wet conditions persisting at Basin Pond over the last 900 years, fire activity has increased. Although recent fire activity is likely anthropogenically triggered (i.e. via land-use change), our results imply a distinct relationship between climate and fire occurrence over the last 900 years in the NE US. Thus, the paleotemperature reconstruction presented here alongside site-specific knowledge from Basin Pond informs our understanding of climatic variability in NE US beyond the era of human influence.



Acknowledgements

The authors thank John Sweeney for his assistance in sediment trap construction and design. Jeff Salacup is acknowledged for technical laboratory assistance. We thank the members of the UMass Biogeochemistry Lab for helpful feedback and discussion. We are grateful to Lucas Groat, Christopher Mode, and Paige Miller-Hughes for their assistance in sediment trap
5 deployment and collection. Dr. Mike Retelle, Dan Frost, Julie Savage, and the Bates College Geology Department are recognized for sediment coring assistance. We are indebted to the Basin-David-Tilton Ponds Association for their cooperation and support. Funding for this project was provided by grant G12AC00001 from the United States Geological Survey and the 2014 and 2015 Joe Hartshorn Memorial Award through the UMass Amherst Department of Geosciences. Results are solely the responsibility of the authors and do not necessarily represent the views of the Northeast Climate Science Center or the
10 USGS.

References

- Anderson, R.S.: Effects of Rotenone on Zooplankton Communities and a Study of their Recovery Patterns in Two Mountain Lakes in Alberta, *Journal of the Fisheries Research Board of Canada*, 27, 1335–1356, 1970.
- Bechtel, A., Smittenberg, R.H., Bernasconi, S.M., and Schubert, C.J.: Distribution of branched and isoprenoid tetraether lipids
15 in an oligotrophic and a eutrophic Swiss lake: Insights into sources and GDGT-based proxies, *Organic Geochemistry*, 41, 822–832, 2010.
- Buckles, L.K., Weijers, J.W.H., Verschuren, D., and Sinninghe Damsté, J.S.: Sources of core and intact branched tetraether membrane lipids in the lacustrine environment: Anatomy of Lake Challa and its catchment, equatorial East Africa, *Geochimica et Cosmochimica Acta*, 140, 106–126, 2014.
- 20 Castañeda, I.S., and Schouten, S.: A review of molecular organic proxies for examining modern and ancient lacustrine environments, *Quaternary Science Reviews* 30, 2851–2891, 2011. doi:10.1016/j.quascirev.2011.07.009.
- Clifford, M.J., and Booth, R.K.: Increased probability of fire during late Holocene droughts in northern New England, *Climatic Change*, 119, 693–704, 2013.
- Colcord, D.E., Cadieux, S.B., Brassell, S.C., Castañeda, I.S., Pratt, L.M., and White, J.R.: Assessment of branched GDGTs as
25 temperature proxies in sedimentary records from several small lakes in southwestern Greenland, *Organic Geochemistry*, 82, 33–41, 2015.
- De Jonge, C., Hopmans, E.C., Stadnitskaia, A., Rijpstra, W.I.C., Hofland, R., Tegelaar, E., and Sinninghe Damsté, J.S.: Identification of novel penta- and hexamethylated branched glycerol dialkyl glycerol tetraethers in peat using HPLC–MS², GC–MS and GC–SMB–MS, *Organic Geochemistry*, 54, 78–82, 2013.
- 30 De Jonge, C., Stadnitskaia, A., Hopmans, E.C., Cherkashov, G., Fedotov, A., Streletskaya, I.D., Vasiliev, A.A., and Sinninghe Damsté, J.S.: Drastic changes in the distribution of branched tetraether lipids in suspended matter and sediments from the



- Yenisei River and Kara Sea (Siberia): Implications for the use of brGDGT-based proxies in coastal marine sediments, *Geochimica et Cosmochimica Acta*, 165, 200–225, 2015.
- Foster, L.C., Pearson, E.J., Juggins, S., Hodgson, D.A., Saunders, K.M., Verleyen, E., and Roberts, S.J.: Development of a regional glycerol dialkyl glycerol tetraether (GDGT)–temperature calibration for Antarctic and sub-Antarctic lakes, *Earth and Planetary Science Letters*, 433, 370–379, 2016.
- Fernholz, E., and MacPhillamy, H.B.: Isolation of a New Phytosterol: Campesterol, *J. Am. Chem. Soc.*, 63, 1155–1156, 1941. doi:10.1021/ja01849a079.
- Frost, D.S.: Paleoclimate Reconstruction using Physical Sedimentology and Organic Matter Biogeochemistry of Varved Sediments, Basin Pond, Fayette, ME (Undergraduate Thesis). Bates College, 2005.
- 10 Gajewski, K.: Late holocene climate changes in eastern North America estimated from pollen data, *Quaternary Research*, 29, 255–262, 1988.
- Gajewski, K., Swain, A.M., and Peterson, G.M.: Late Holocene Pollen Stratigraphy in Four Northeastern United States Lakes, *Géographie physique et Quaternaire*, 41, 377, 1987.
- Gao, L., Huang, Y., Shuman, B., Oswald, W.W., and Foster, D.: A high-resolution hydrogen isotope record of behenic acid
15 for the past 16 kyr in the northeastern United States, *Quaternary International*, 449, 1–11, 2017.
- Hopmans, E.C., Schouten, S., and Sinninghe Damsté, J.S.: The effect of improved chromatography on GDGT-based palaeoproxies, *Organic Geochemistry*, 93, 1–6, 2016.
- Hopmans, E.C., Weijers, J.W.H., Schefuß, E., Herfort, L., Sinninghe Damsté, J.S., and Schouten, S.: A novel proxy for terrestrial organic matter in sediments based on branched and isoprenoid tetraether lipids, *Earth and Planetary Science Letters*,
20 224, 107–116, 2004.
- Horton, R., Yohe, G., Easterling, W., Kates, R., Ruth, M., Sussman, E., Whelchel, A., Wolfe, D., and Lipschultz, F.: Ch. 16: Northeast. Climate Change Impacts in the United States: The Third National Climate Assessment, 2014. doi:10.7930/J0SF2T3P
- Hou, J., D’Andrea, W.J., and Huang, Y.: Can sedimentary leaf waxes record D/H ratios of continental precipitation? Field,
25 model, and experimental assessments. *Geochimica et Cosmochimica Acta*, 72, 3503–3517, 2008.
- Kiser, R.W., Donaldson, J.R., and Olson, P.R.: The Effect of Rotenone on Zooplankton Populations in Freshwater Lakes, *Transactions of the American Fisheries Society*, 92, 17–24, 1963.
- Klok, J., Baas, M., Cox, H.C., de Leeuw, J.W., and Schenck, P.A.: Loliolides in dihydroactinidiolide in a recent marine sediment probably indicate a major transformation pathway of carotenoids, *Tetrahedron Letters*, 25, 5577–5580, 1984.
- 30 Köster, D., Pienitz, R., Wolfe, B.B., Barry, S., Foster, D.R., and Dixit, S.S.: Paleolimnological assessment of human-induced impacts on Walden Pond (Massachusetts, USA) using diatoms and stable isotopes, *Aquatic Ecosystem Health & Management*, 8, 117–131, 2005.
- Kunkel, K.E.: Regional climate trends and scenarios for the US National Climate Assessment, US Department of Commerce, National Oceanic and Atmospheric Administration, National Environmental Satellite, Data, and Information Service, 2013.



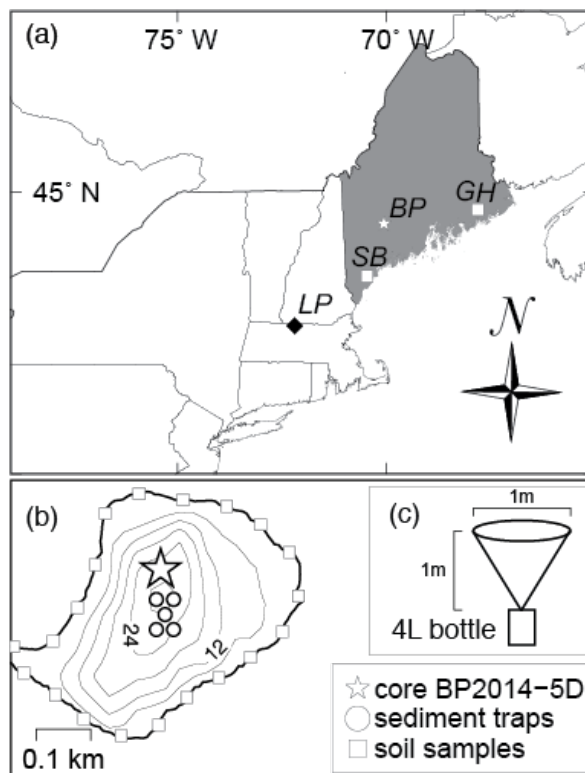
- Loomis, S.E., Russell, J.M., Heurix, A.M., D'Andrea, W.J., and Sinninghe Damsté, J.S.: Seasonal variability of branched glycerol dialkyl glycerol tetraethers (brGDGTs) in a temperate lake system, *Geochimica et Cosmochimica Acta*, 144, 173–187, 2014.
- Loomis, S.E., Russell, J.M., Ladd, B., Street-Perrott, F.A., and Sinninghe Damsté, J.S.: Calibration and application of the branched GDGT temperature proxy on East African lake sediments, *Earth and Planetary Science Letters*, 357–358, 277–288, 2012.
- Marlon, J.R., Pederson, N., Nolan, C., Goring, S., Shuman, B., Robertson, A., Booth, R., Bartlein, P.J., Berke, M.A., Clifford, M., Cook, E., Dieffenbacher-Krall, A., Dietze, M.C., Hessl, A., Hubeny, J.B., Jackson, S.T., Marsicek, J., McLachlan, J., Mock, C.J., Moore, D.J.P., Nichols, J., Peteet, D., Schaefer, K., Trouet, V., Umbanhowar, C., Williams, J.W., and Yu, Z.: Climatic history of the northeastern United States during the past 3000 years, *Clim. Past*, 13, 1355–1379, 2017.
- Meyers, S.R.: Seeing red in cyclic stratigraphy: Spectral noise estimation for astrochronology, *Paleoceanography*, 27, PA3228, 2012.
- Miller, D.R., Castañeda, I.S., Bradley, R.S., and MacDonald, D.: Local and regional wildfire activity in central Maine (USA) during the past 900 years, *Journal of Paleolimnology*, 58, 455–466, 2017.
- Myrbo, A.: Sedimentary and historical context of eutrophication and remediation in urban Lake McCarrons (Roseville, Minnesota), *Lake and Reservoir Management*, 24, 349–360, 2008.
- Ortega, P., Lehner, F., Swingedouw, D., Masson-Delmotte, V., Raible, C.C., Casado, M., and Yiou, P.: A model-tested North Atlantic Oscillation reconstruction for the past millennium, *Nature*, 523, 71–74, 2015.
- O'Sullivan, P.E.: Annually-laminated lake sediments and the study of Quaternary environmental changes — a review, *Quaternary Science Reviews*, 1, 245–313, 1983.
- PAGES 2k Consortium: Continental-scale temperature variability during the past two millennia, *Nature Geoscience*, 6, 339–346, 2013.
- Pearson, E.J., Juggins, S., Talbot, H.M., Weckström, J., Rosén, P., Ryves, D.B., Roberts, S.J., and Schmidt, R.: A lacustrine GDGT-temperature calibration from the Scandinavian Arctic to Antarctic: Renewed potential for the application of GDGT-paleothermometry in lakes, *Geochimica et Cosmochimica Acta*, 75, 6225–6238, 2011.
- Peterse, F., van der Meer, J., Schouten, S., Weijers, J.W.H., Fierer, N., Jackson, R.B., Kim, J.-H., and Sinninghe Damsté, J.S.: Revised calibration of the MBT–CBT paleotemperature proxy based on branched tetraether membrane lipids in surface soils, *Geochimica et Cosmochimica Acta*, 96, 215–229, 2012.
- Repeta, D.J.: Carotenoid diagenesis in recent marine sediments: II. Degradation of fucoxanthin to loliolide, *Geochimica et Cosmochimica Acta*, 53, 699–707, 1989.
- Russell, J.M., Hopmans, E.C., Loomis, S.E., Liang, J., and Sinninghe Damsté, J.S.: Distributions of 5- and 6-methyl branched glycerol dialkyl glycerol tetraethers (brGDGTs) in East African lake sediment: Effects of temperature, pH, and new lacustrine paleotemperature calibrations, *Organic Geochemistry*, 117, 56–69, 2018.



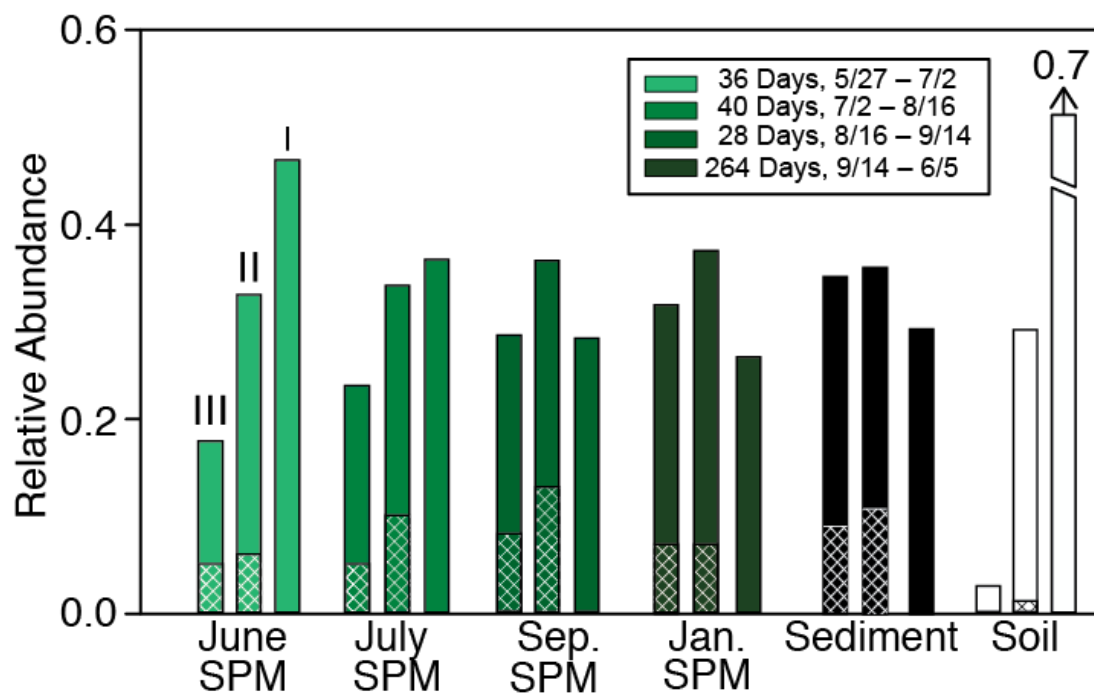
- Sachse, D., Billault, I., Bowen, G.J., Chikaraishi, Y., Dawson, T.E., Feakins, S.J., Freeman, K.H., Magill, C.R., McInerney, F.A., Meer, M.T.J. van der, Polissar, P., Robins, R.J., Sachs, J.P., Schmidt, H.-L., Sessions, A.L., White, J.W.C., West, J.B., and Kahmen, A.: Molecular Paleohydrology: Interpreting the Hydrogen-Isotopic Composition of Lipid Biomarkers from Photosynthesizing Organisms, *Annual Review of Earth and Planetary Sciences*, 40, 221-249, 2012.
- 5 Sanni, S., and Wærnvågen, S.B.: Oligotrophication as a result of planktivorous fish removal with rotenone in the small, eutrophic, Lake Mosvatn, Norway, *Hydrobiologia*, 200-201, 263–274, 1990.
- Schoon, P.L., de Kluijver, A., Middelburg, J.J., Downing, J.A., Sinninghe Damsté, J.S., and Schouten, S.: Influence of lake water pH and alkalinity on the distribution of core and intact polar branched glycerol dialkyl glycerol tetraethers (GDGTs) in lakes, *Organic Geochemistry*, 60, 72–82, 2013.
- 10 Sinninghe Damsté, J.S., Ossebaar, J., Abbas, B., Schouten, S., and Verschuren, D.: Fluxes and distribution of tetraether lipids in an equatorial African lake: Constraints on the application of the TEX86 palaeothermometer and BIT index in lacustrine settings, *Geochimica et Cosmochimica Acta*, 73, 4232–4249, 2009.
- Sinninghe Damsté, J.S., Rijpstra, W.I.C., Hopmans, E.C., Weijers, J.W.H., Foesel, B.U., Overmann, J., and Dedysh, S.N.: 13,16-Dimethyl Octacosanedioic Acid (iso-Diabolic Acid), a Common Membrane-Spanning Lipid of Acidobacteria
- 15 Subdivisions 1 and 3, *Applied and Environmental Microbiology*, 77, 4147–4154, 2011.
- Sinninghe Damsté, J.S., Ossebaar, J., Schouten, S., and Verschuren, D.: Distribution of tetraether lipids in the 25-ka sedimentary record of Lake Challa: extracting reliable TEX86 and MBT'5ME/CBT palaeotemperatures from an equatorial African lake, *Quaternary Science Reviews*, 50, 43–54, 2012.
- Sun, C., Li, J., and Jin, F.-F.: A delayed oscillator model for the quasi-periodic multidecadal variability of the NAO, *Climate*
- 20 *Dynamics*, 45, 2083–2099, 2015.
- Sun, Q., Chu, G., Liu, M., Xie, M., Li, S., Ling, Y., Wang, X., Shi, L., Jia, G., and Lü, H.: Distributions and temperature dependence of branched glycerol dialkyl glycerol tetraethers in recent lacustrine sediments from China and Nepal, *Journal of Geophysical Research*, 116, 2011. doi:10.1029/2010JG001365
- Tierney, J.E., and Russell, J.M.: Distributions of branched GDGTs in a tropical lake system: Implications for lacustrine
- 25 application of the MBT/CBT paleoproxy, *Organic Geochemistry*, 40, 1032–1036, 2009.
- Tierney, J.E., Russell, J.M., Eggermont, H., Hopmans, E.C., Verschuren, D., and Sinninghe Damsté, J.S.: Environmental controls on branched tetraether lipid distributions in tropical East African lake sediments, *Geochimica et Cosmochimica Acta*, 74, 4902–4918, 2010.
- Tierney, J.E., Schouten, S., Pitcher, A., Hopmans, E.C., and Sinninghe Damsté, J.S.: Core and intact polar glycerol dialkyl
- 30 glycerol tetraethers (GDGTs) in Sand Pond, Warwick, Rhode Island (USA): Insights into the origin of lacustrine GDGTs, *Geochimica et Cosmochimica Acta*, 77, 561–581, 2012.
- Trenberth, K., Zhang, R., & National Center for Atmospheric Research Staff (Eds): *The Climate Data Guide: Atlantic Multi-decadal Oscillation (AMO)*, Retrieved from <https://climatedataguide.ucar.edu/climate-data/atlantic-multi-decadal-oscillation-amo>, 2017.



- Volkman, J.K.: A review of sterol markers for marine and terrigenous organic matter, *Organic Geochemistry*, 9, 83–99, 1986. doi:10.1016/0146-6380(86)90089-6.
- Volkman, J.K., Barrett, S.M., Blackburn, S.I., Mansour, M.P., Sikes, E.L., and Gelin, F.: Microalgal biomarkers: A review of recent research developments, *Organic Geochemistry*, 29, 1163–1179, 1998. doi:10.1016/S0146-6380(98)00062-X.
- 5 Volkman, J.: Sterols in microorganisms, *Appl Microbiol Biotechnol*, 60, 495–506, 2003. doi:10.1007/s00253-002-1172-8.
- Wang, H., Liu, W., Zhang, C.L., Wang, Z., Wang, J., Liu, Z., and Dong, H.: Distribution of glycerol dialkyl glycerol tetraethers in surface sediments of Lake Qinghai and surrounding soil, *Organic Geochemistry*, 47, 78–87, 2012.
- Webb, T., Shuman, B., Leduc, P., Newby, P., and Miller, N.: Late Quaternary climate history of western New York State, *Bulletin of the Buffalo Society of Natural Sciences*, 37, 11–13, 2003.
- 10 Weber, Y., De Jonge, C., Rijpstra, W.I.C., Hopmans, E.C., Stadnitskaia, A., Schubert, C.J., Lehmann, M.F., Sinninghe Damsté, J.S., and Niemann, H.: Identification and carbon isotope composition of a novel branched GDGT isomer in lake sediments: Evidence for lacustrine branched GDGT production, *Geochimica et Cosmochimica Acta*, 154, 118–129, 2015.
- Weijers, J.W.H., Schouten, S., van den Donker, J.C., Hopmans, E.C., and Sinninghe Damsté, J.S.: Environmental controls on bacterial tetraether membrane lipid distribution in soils, *Geochimica et Cosmochimica Acta*, 71, 703–713, 2007.
- 15 Wetzel, A.: Biogenic structures in modern slope to deep-sea sediments in the Sulu Sea Basin (Philippines), *Palaeogeography, Palaeoclimatology, Palaeoecology*, 42, 285–304, 1983.
- Zell, C., Kim, J.-H., Moreira-Turcq, P., Abril, G., Hopmans, E.C., Bonnet, M.-P., Sobrinho, R.L., and Sinninghe Damsté, J.S.: Disentangling the origins of branched tetraether lipids and crenarchaeol in the lower Amazon River: Implications for GDGT-based proxies, *Limnology and Oceanography*, 58, 343–353, 2013.
- 20 Zhu, C., Weijers, J.W.H., Wagner, T., Pan, J.-M., Chen, J.-F., and Pancost, R.D.: Sources and distributions of tetraether lipids in surface sediments across a large river-dominated continental margin, *Organic Geochemistry*, 42, 376–386, 2011.
- Zink, K.-G., Vandergoes, M.J., Mangelsdorf, K., Dieffenbacher-Krall, A.C., and Schwark, L.: Application of bacterial glycerol dialkyl glycerol tetraethers (GDGTs) to develop modern and past temperature estimates from New Zealand lakes, *Organic Geochemistry, Advances in Organic Geochemistry 2009 Proceedings of the 24th International Meeting on Organic*
- 25 *Geochemistry*, 41(9), 1060–1066, 2010.



5 **Figure 1. Map of Basin Pond. (a)** The location of Basin Pond (BP) (white star) in Maine, USA. Locations of three other sites are labelled: Little Pond (LP; Gao et al. 2017), Great Heath Lake (GH; Nichols and Huang, 2012; Clifford and Booth, 2013), and Saco Bog (SB; Clifford and Booth, 2013). For more information regarding these sites, see Supplementary Information. **(b)** Bathymetric profile (6 m contours) of Basin Pond with position of floating sediment traps (circles), surface soil samples (squares), and core BD-2014-5D used for the downcore temperature reconstruction in this study (star). The pond has an area of approximately 0.14 km². **(c)** Schematic of sediment traps utilized in this study.



5 Figure 2. Temporal variation of the relative abundance of groups I, II and III brGDGTs in SPM (green shaded bars), sediment (black bars), and catchment soil samples (white bars). Sediment and soil samples were collected in Spring of 2014. Green shaded bars for SPM samples reflect averages for each date samples were collected, measured in July 2014 (lightest green), August 2014, September 2014 and June 2015 (darkest green). For each category, brGDGT groups III, II, and I are shown in that order (left to right). Lines in each bar represent the relative abundance of 5- and 6- methyl brGDGTs, with cross hatching representing 6- methyl abundances.

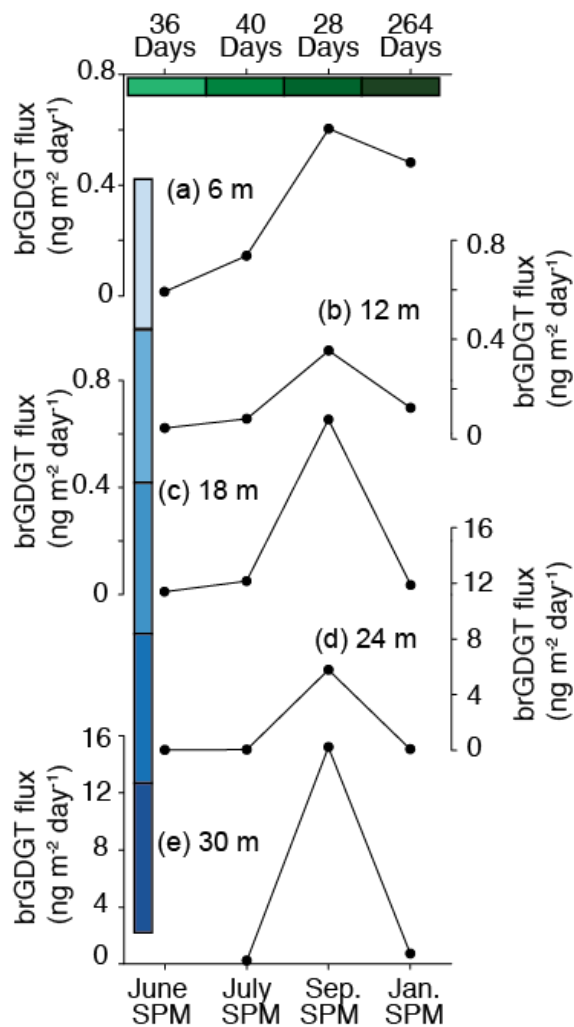
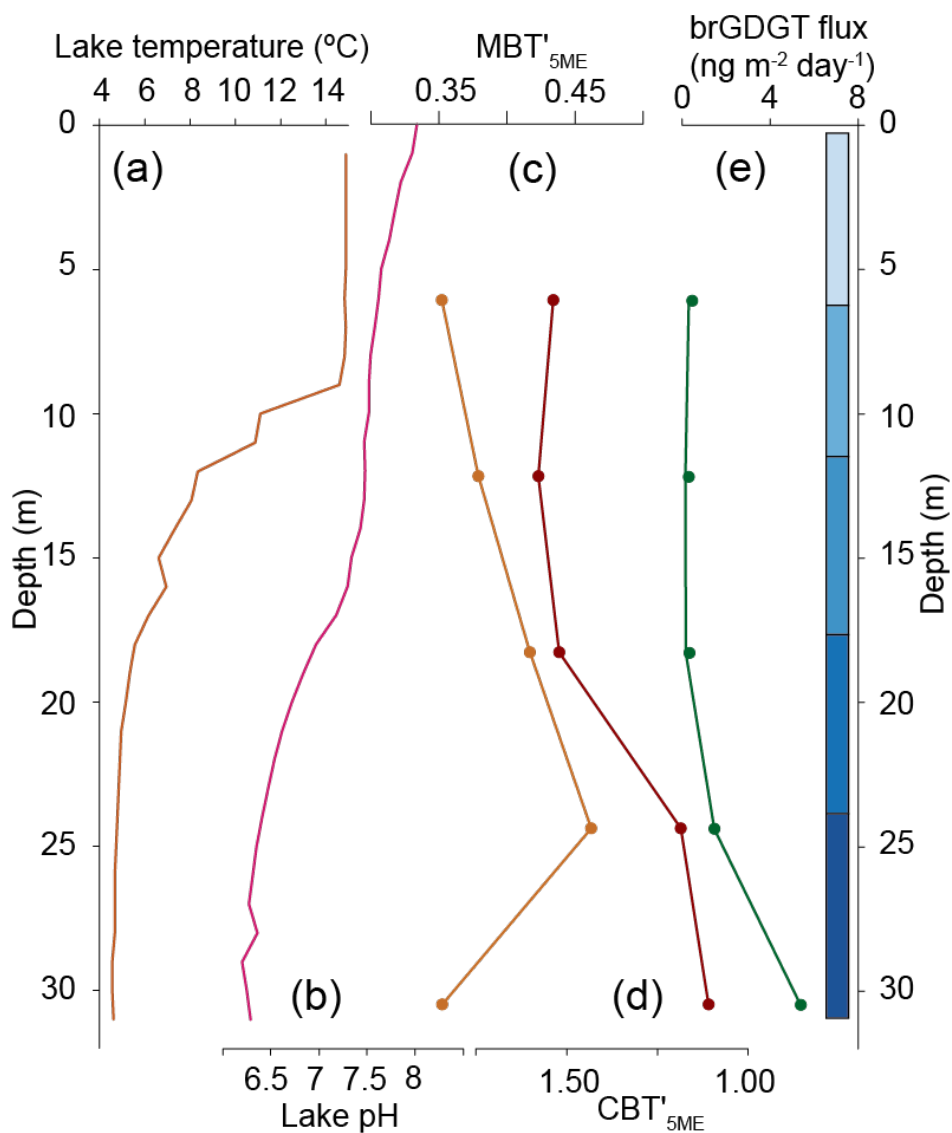
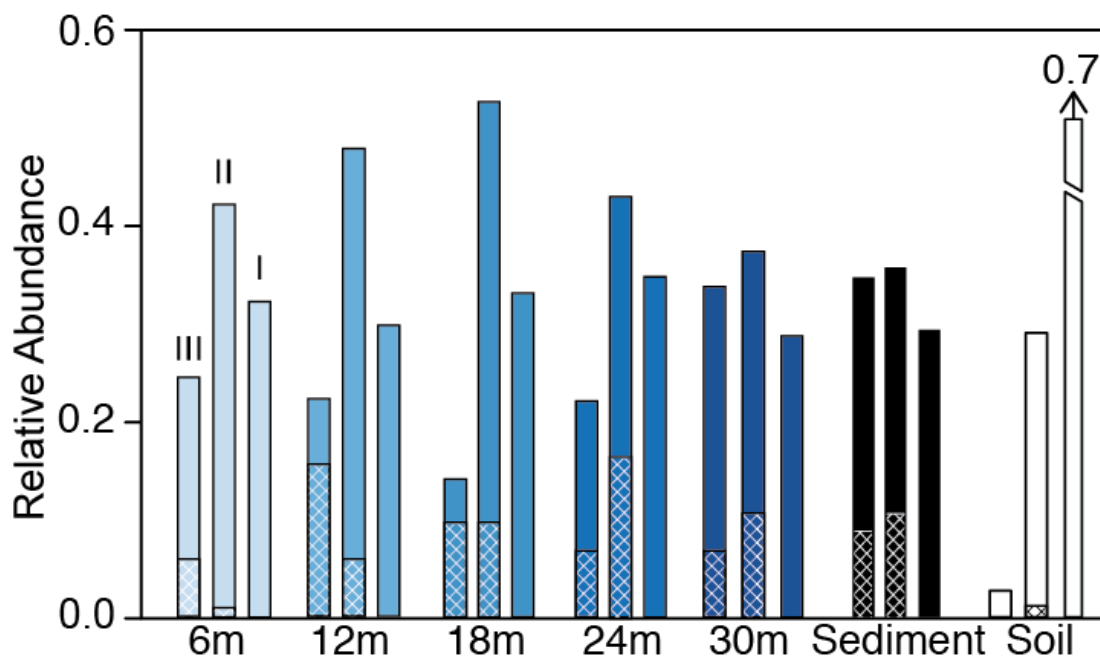


Figure 3. Time series of brGDGT fluxes for each of the sediment traps in Basin Pond. brGDGT fluxes at 6m (a), 12m (b), 18m (c), 24m (d), and 30m (e) are shown. There is no data for trap (e) in July 2014. Note the change of scale for (d) and (e), indicating fluxes an order of magnitude higher for the lowermost traps. Green bars correspond to the time periods in Figure 2. Blue bars correspond to the depth ranges in Figure 5.

5



5 **Figure 4.** Hydrolab-measured temperature and pH profiles for Basin Pond compared with brGDGT-based reconstructions. (a) Fall lake temperature profile, showing the mixed layer extending to ~9 m water depth, followed by the thermocline (9-15 m) and a cold deep layer (15-32 m). (b) Fall pH profile. the pH ranges from ~7.5 at the surface to ~6.2 at depth. (c) Average MBT values measured at sediment traps. (d) Average CBT values measured at sediment traps. (e) brGDGT fluxes measured at sediment traps.



5 Figure 5. Spatial variation in the water column of the relative abundance of groups I, II and III brGDGTs in SPM as a function of water depth. For each group, the relative abundance at depths of 6 m (lightest blue), 12 m, 18 m, 24 m, and 30 m (darkest blue) is plotted next to the average surface sediment (black) and catchment soil (white). For each category, brGDGT groups III, II, and I are shown in that order (left to right). Lines in each bar represent the relative abundance of 5- and 6- methyl brGDGTs, with cross hatching representing 6- methyl abundances.

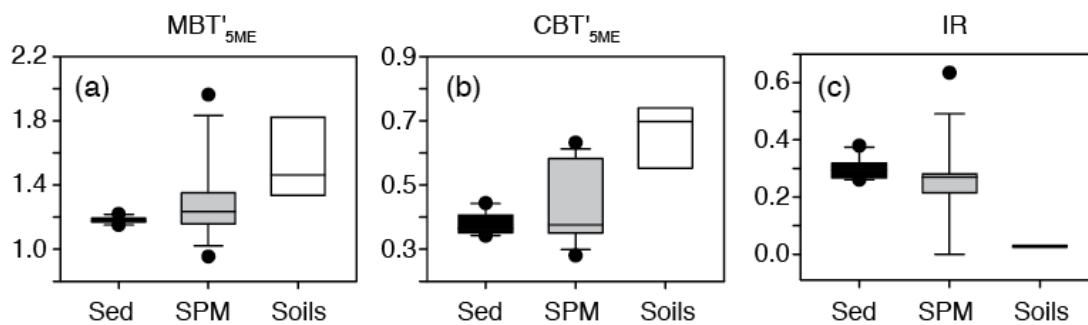


Figure 6. BrGDGT-based proxies measured on surface sediments (black), SPM (gray), and catchment soils (white). (a) Cyclization of Branched Tetraethers (CBT), (b) Methylation of branched tetraethers (MBT'_{5ME}), and (c) the Isomer Ratio (IR).

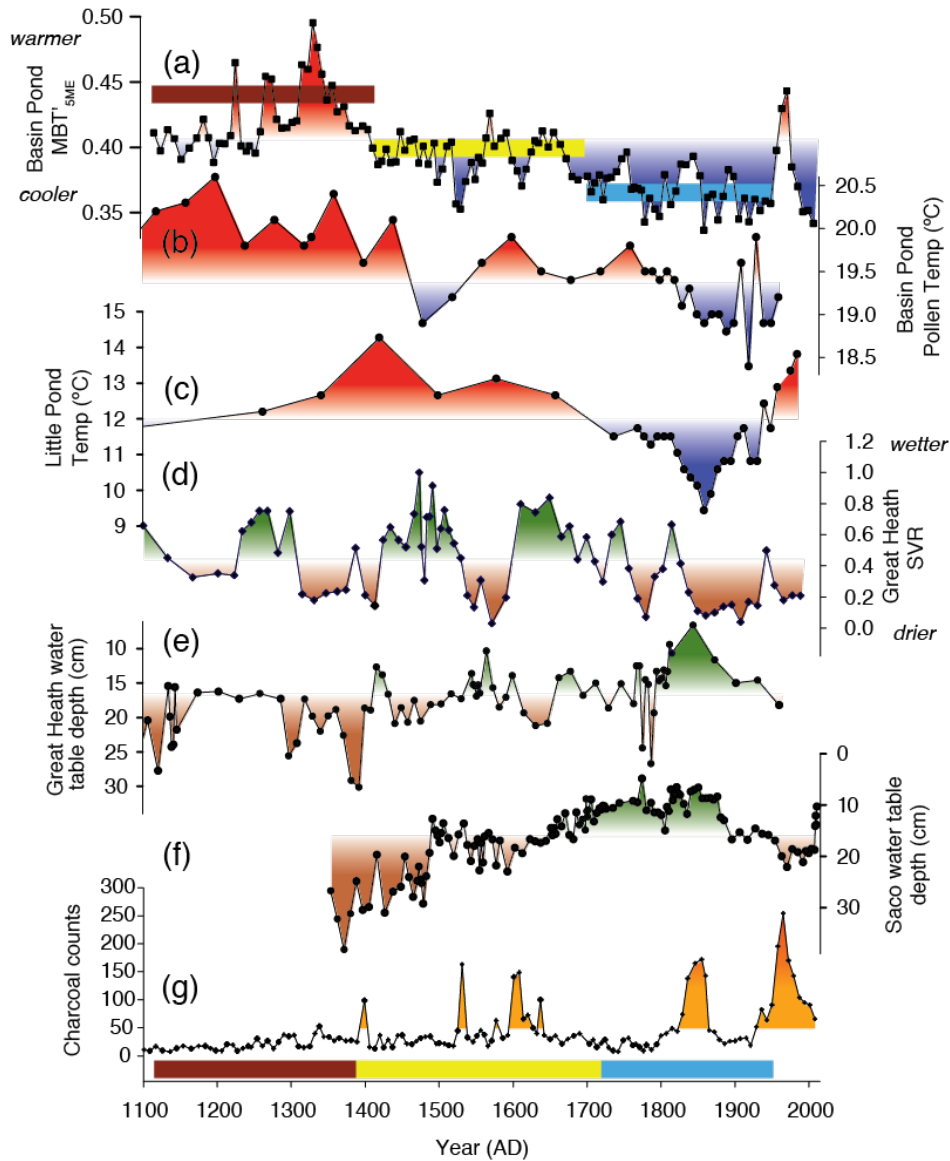
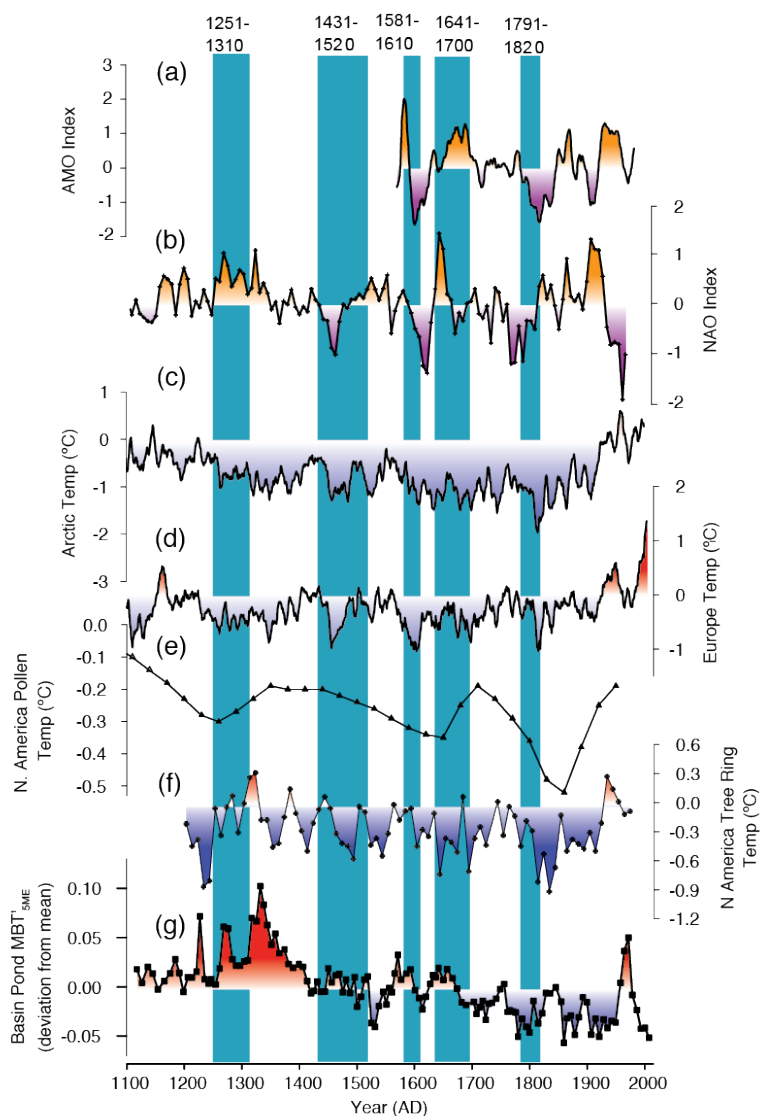


Figure 7. The Basin Pond MBT record compared with other paleoclimate records from the NE US. (a) MBT (this study). Colored bars indicate the three main periods discussed in the text. (b) Pollen-based reconstruction of temperature at Basin Pond (Gajewski, 1988). (c) Deuterium isotope (δD)-based reconstruction of temperature at Little Pond (Gao et al., 2017). (d) Great Heath aridity reconstruction based on the *Sphagnum/Vascular Ratio* (SVR) (Nichols and Huang, 2012). (e) Water table reconstruction from Great Heath (Clifford and Booth, 2013). (f) Water table reconstruction from Saco Bog (Clifford and Booth, 2013). (g) Charcoal counts from Basin Pond (Miller et al., 2017).

5



5 **Figure 8.** The Basin Pond MBT'_{SME} record compared with regional and global records of temperature change. (a) Tree-ring based reconstruction of the AMO Index (Gray et al., 2004). (b) NAO Index reconstruction (Sun et al., 2015). (c–f) Regional temperature stacks based on composite proxy reconstructions for the Arctic (c), Europe (d), and North America (pollen, (e); tree rings, (f)). The records have been standardized to have the same mean (0) and standard deviation (1) from 1190–1970 AD (PAGES2k 2013). (g) MBT'_{SME} (this study).

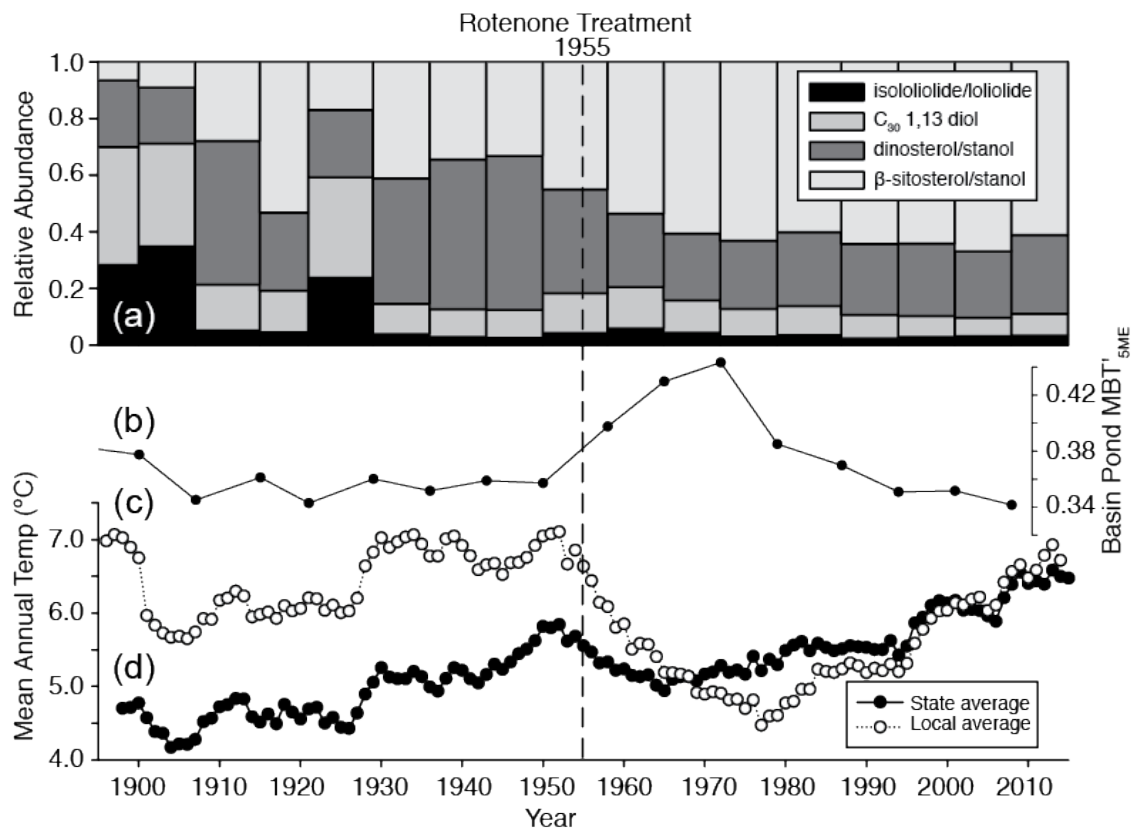


Figure 9. Comparison of regional historical temperature records for Maine (state and local temperature), MBT_{5ME} reconstruction, and algal lipid biomarkers in Basin Pond. (a) Relative abundance of four major algal lipids. (b) MBT_{5ME} record. (c) Local temperature measured at Farmington and Livermore Falls meteorological stations. (d) Maine statewide average temperature (NOAA, 2014). The black line indicates the rotenone treatment of the lake in 1955.

5